Full Length Research Paper

The effect of *mucA* allele on biofilm architecture and the biofilm-related proteomes

Anqun Chen[1], Linka Xie[2], Ming Ni[2], Mathee Kalai[3] and Deying Tian[2]*

[1]Department of Nephrology, the first affiliated hospital of Chongqing Medical university, ChongQing 400016, China.
[2]Department of Infectious Disease, TongJi Hospital, TongJi Medical College of HuaZhong University of Science and Technology, WuHan 430030, China.
[3]Florida International University, University Park Campus, MARC 430, Miami, FL 33199, USA.

In this study, a unique mucA mutation (designated mucA56) was introduced, which was characterized by deletion of bases 166-333, encoding MucA56 protein with the deletion of the trans-membrane region, which then was proved to be cytoplasmic with *phoA-mucA* fusion method. PAOmucA56 was constructed with homologous recombination; two PAO1 derivatives PAOmucA22 (PDO300) and PAOmucA56 displayed mucoid phenotype on pseudomonas isolation agar (PIA) agar, but PDO300 produced more alginate than PAOmucA56. Scanning confocal laser microscopy was used to observe the biofilm structures of the three strains during various biofilm development stages. PDO300 developed biofilm with low substratum coverage and high structural heterogeneity, while PAOmucA56 and PAO1 formed uniform biofilm with complete substratum coverage. The proteomes of crude protein extracts of biofilm cells revealed that there are 17 candidate proteins differentially expressed between the two kinds of biofilm, which were proteins involved in protein synthesis, MucA degradation, energy metabolism, carbon catabolism and amino acid metabolism and so on. We might conclude that alginate production may affect biofilm architecture, and proteins involved in protein synthesis, MucA degradation, energy metabolism, carbon catabolism and amino acid metabolism might play a role in biofilm development alternatively.

Key words: *Pseudomonas aeruginosa,* mucA, alginate, biofilm, proteome.

INTRODUCTION

Pseudomonas aeruginosa is a ubiquitous Gram-negative bacterium frequent in soil and water environments. It has become one of the most common and deadly opportunistic pathogens, causing nosocomial pneumonia, catheter and urinary tract infections, sepsis in burn wound and immunocompromised patients (Stover et al., 2000). A diverse set of adaptive responses allows *P. aeruginosa* to establish this wide range of infections. An important adaptation to pulmonary pathogenesis by *P. aeruginosa* is the emergence of mucoid variants of the original strain (Firoved and Deretic, 2003). Infections of mucoid *P. aeruginosa characterized with constitutive alginate expression* are virtually impossible to eradicate.

Alginate expression is regulated by the extracytoplasmic function (ECF) σ factor AlgU (also named AlgT or σ^{22} and similar to the σ^E of *Escherichia coli*) and its cognate anti-σ factor MucA, which negatively regulates the expression of alginate by binding to AlgU (Deretic et al., 1994). The signal transduction pathway, which communicates information from the cell envelope to σ^E in the cytoplasm, is related to a widely conserved prokaryotic and eukaryotic mechanism called Regulated Intra-membrane Proteolysis or RIP (Chaba et al., 2007). In *E. coli* right after the initiation of the RIP stress response, inner membrane proteases DegS and YaeL act sequentially to degrade membrane bound RseA, an anti-sigma factor that binds σ^E, thus releasing σ^E in stressed cells (Alba and Gross, 2004). In *P. aeruginosa,* MucA binds to σ^{22} in the inner membrane, thus preventing its interaction with promoters and RNA polymerase, which keeps alginate promoter (P_{algD}) nearly silent. In wild-type *P. aeruginosa,*

*Corresponding author. E-mail: dytian@tjh.tjmu.edu.cn. Tel: +86-27-83662816. Fax: +86-27-83662816.

cell wall stress (for example, peptidoglycan inhibitors and misfolded porins) activate a RIP cascade in which the AlgW and YaeL/MucP proteases degrade MucA to release σ^{22}, thus allowing P_{algD} expression (Qiu et al., 2007). In a certain environment, there is a selection for *mucA* mutations that make MucA defective, thus releasing σ^{22} to allow maximal expression of P_{algD} (Ohman, 2009). The wild-type MucA protein (like *E. coli* RseA) is an inner-membrane protein of 194 amino acids (aa) that might have three functional domains: $MucA_{7-57}$ (equivalent to the N-terminal region of RseA), which has been proposed to be located in the cytoplasm, $MucA_{84-104}$, which has been shown to contain a transmembrane domain, and $MucA_{113-170}$ (equivalent to the C-terminal region of RseA), which might be located in the periplasm (Qiu et al., 2008).

Any mutation that can free the stress-response sigma factor AlgU from negative regulation by the anti-sigma factor MucA can lead to conversion to mucoidy (Firoved and Deretic, 2003). Mutations in *mucA* of the *algU mucABCD* operon are a major cause of conversion to the mucoid phenotype in clinical and laboratory isolates (Qiu et al., 2007). More than 80% of the frameshift or nonsense mutations that give rise to a premature stop signal are clustered within the 100 bp stretch from nt 340–439 of the 585 bp of the mucA gene. The most common *mucA22* allele is characterized by a single base pair deletion at position 430, and it accounts for 40% of all stop mutations (Bragonzi et al., 2006). We isolated a mucoid strain from a patient who suffered from repeated pulmonary infection, which contained a previously unreported *mucA* allele (designated *mucA56*) characterized by a deletion of bases 166 to 333, and its sequence in Genebank is AY608668. *MucA56* allele encodes an incomplete polypeptide of 138 aa with a deletion of 56 aa ($MucA_{54-110}$). This protein is located in the cytoplasm due to the absence of the transmembrane domain ($MucA_{84-104}$), which was proved by *mucA-phoA* fusion method. The widely used laboratory mucoid strain PDO300 (PAO*mucA22*) encodes a 146 aa MucA polypeptide with a C-terminal truncation, which is located in the membrane. Both *mucA* mutations can free the stress response sigma factor AlgU from negative regulation by the anti-σ factor MucA, but they differ with regard to protein subcellular localization and structure. We found that both PDO300 and PAOmucA56 displayed mucoid phenotype on PIA agar, but PDO300 looked more mucoidy, and produced more alginate than PAOmucA56. A scanning confocal laser microscopy was used to observe the biofilm structures of the three strains during various biofilm development stages. It turned out that PAO1 and PAO*mucA56* developed from a uniform monolayer of attached cells into mature biofilms with an almost complete substratum coverage and even biomass distribution. However, PDO300 formed significantly different biofilm architecture, with attached cells growing exclusively in discrete micro-colonies, resulting in a low substratum coverage and high structural heterogeneity.

Further proteome research revealed that there are 17 candidate proteins possibly contributing to the distinguished biofilm, which are proteins involved in protein synthesis, MucA degradation, energy metabolism, carbon catabolism and amino acid metabolism and so on.

MATERIALS AND METHODS

Bacterial strains, plasmids and media

The strains and plasmids used in this study are listed in Table 1. Planktonic strains were cultured by shaking at 37°C overnight in Luria broth (LB) with antibiotics when necessary. LB with appropriate antibiotic was used to grow cells in continuous-flow reactors. LA/PIA, used in biparental matings, was a 1:1 mix of pseudomonas isolation agar (Difco) and L agar. Sucrose sensitivity was tested on L agar plates containing 5% sucrose. Antibiotics were used at the following concentrations (µg/ml): ampicillin, 100; kanamycin, 30; carbenicillin, 300. L agar containing 5-bromo-4-chloro-3-indolyl phosphate (XP) at 40 mg/ml was used for the colonies selection containing active fusions.

Construction of *mucA56*-phoA fusion

The *mucA56* gene isolated from a patient as aforementioned, was amlified from PA17 with *NcoI* and *XbaI* restrictive endonucleases and cloned into pMF54 expression vector, resulting in pCAQ56. Alkaline phosphatase gene, obtained from pPHO7 by use of *XbaI*, was fused to the *mucA56* in pCAQ56, resulting in the *mucA56-phoA* fusion expression vector pCAQ57. Gene fusion vector pCAQ57 was confirmed first by PCR and sequencing, then by western blot using anti-alkaline phosphatase antibody. pCAQ57, pKMG170 (negative control plasmid) and pKMG176 (positive control plasmid) were transformed into PAO1. Colonies containing active fusions were screened for blue color on L agar containing 5-bromo-4-chloro-3-indolyl phosphate (XP) at 40 mg/ml.

Construction of a *mucA56* mutant of *P. aeruginosa* PAO1

Plasmid pEX100T-mucA56 was formed by cloning a 2.0 kb *SmaI* DNA fragment from PA17 into the blunt-end *SmaI* site of pEX100T, which is a mobilizable suicide plasmid containing a *sacB* gene that confers sucrose sensitivity in *P. aeruginosa*. This plasmid was transferred into strain PAO1 from *E. coli* with biparental mating, and the merodiploids that formed by homologous recombination with the chromosome were selected with 300 µg/ml carbenicillin. Such strains were then grown without selection to permit the occurrence of a second cross-over, which excised the plasmid and left the mutant allele in the chromosome. Colonies appearing on agar plates containing sucrose to select for loss of the plasmid encoding *sacB* were screened for the mucoid phenotype and carbenicillin sensitivity. The presence of *mucA56* mutation in one mucoid derivative was confirmed by PCR and DNA sequencing.

The phenotype of strains and determination of alginate concentration

The *P. aeruginosa* strains (PAO1, PAOmucA56 and PDO300) were streaked into PIA agar, and the phenotype was observed. The production of alginate was determined using a borate/carbazole method (Knutson and Jeanes, 1968) with D-mannuronate lactone (Sigma) used to calibrate a standard curve. The procedure was as

Table 1. Strains and plasmids used in this study.

Strain or plasmid	Phenotype, genotype	Source
PAO1	prototroph	Holloway(1986)
PDO300	Mucoid PAO1 derivative *mucA22*	Mathee (1999)
PA17	Mucoid clinic isolates with the deletion of bases 166-333 in *mucA*	This study
PAO*mucA56*	Mucoid PAO1 derivative	This study
pMF54	pKK233-2 (Ptrc Apr) oriVSF oriT (RK2) lacIq	Mathee (1997)
pPHO7	P15A oriV (Tcr) with MCS-phoA	Mathee (1997)
pKMG170	pMF54-*mucA*(1-54)-phoA	Mathee (1997)
pKMG176	pMF54-*mucA*(1-143)-phoA	Mathee (1997)
pEX100T	pseudomonas suicide vector, sacB, oriT, Cb^R	Mathee (1999)
PCAQ56	pMF54-*mucA56*	This study
PCAQ57	pMF54-*mucA56-phoA*	This study
pUCP20	E.coli-pseudomonas shuttle vector , ori1600P$_{lac}$, Ap^R	Schweizer
pMD18-T	TA cloning vector, ori, Ap^R, P$_{lacZ,}$T-cloning site	TAKARA
pGFPuv	pUCoriP$_{lac}$, Enhanced GFP expression, MCS, Ap^R	Clontech
pGFPuv20	pUCP20 with GFPuv(736bp) from pGFPuv	This study

described by Mathee et al. (1999).

Electrotransformation, biofilm mode of growth and microscopy

An enhanced GFP expression plasmid (pGFPuv20) was constructed by cloning a 736 bp *EcoR* I-*Hind* III fragment from plasmid pGFPuv, into *EcoR* I *Hind* III digested pUCP20, according to the method of Davies et al. (1998). pGFPuv20 was transformed into *P. aeruginosa* by electroporation according to Stapper et al. (2004). A continuous-flow reactor was designed according to Karin et al. (2002), but with small changes. Briefly, medium was pumped through the tubing via a BT100L- DG-4 pump to a closed effluent medium reservoir. The tubes within which the biofilms were cultivated had a regular geometry throughout (2.4 × 0.8 mm), and each was ligated to a u-slide IV flow kit (ibidi) that can be used for in-line microscopic evaluation of biofilm morphology. Noninvasive monitoring of the biofilm's three-dimensional structure was achieved by scanning confocal laser microscopy (SCLM) using an OLYMPUS FV500 system. The 488 nm laser lines of an ArKr laser were used to excite green fluorescent proteins (GFP).

Preparation of crude protein extract

Pseudomonas strains were cultured in a continuous-flow reactor as described previously (Stapper et al., 2004). 20 ml of a tube-grown culture of *P. aeruginosa* was injected through the tubing wall and into the lumen, and allowed to attach for 2 h before the flow of Luria broth (0.5 ml/min) was initiated. After various times (1, 3 and 5 days), biofilm cells were harvested from the interior surface by pinching the tube along its entire length, resulting in extrusion of the cell material from the lumen. The crude protein of biofilm cells was extracted according to Zhang et al. (2008). Experiments for each time point were repeated at least three times.

Two-dimensional gel electrophoresis

1000 µg total cell protein was loaded onto GE Healthcare 18 cm IPG strips (pH 4–7 NL,GE Healthcare) according to Zhang et al. (2008). Proteins were detected by Coomassie brilliant blue staining

and scanned at 300 dpi (PowerLook 2100XL, UMAX company). Image elaboration and analysis were carried out with ImageMaster 2-D Platinum version 5 software (GE Healthcare; Amersham Biosciences). Two-dimensional gels were repeated for each growth condition independently three times to confirm the reproducibility of the protein pattern under attached growth conditions. Only the differences in protein spots that were reproduced three times are described here.

**In-gel digestion and protein identification by MALDI-TOF MS**

This procedure was performed according to the previously described method of Yang et al. (2007). The list of peptide masses from each peptide map fingerprinting (PMF) was saved for database analysis. Peptide mass fingerprints generated by MASCOT software were searched against the NCBI (http://www.ncbi.nlm.nih.gov/database/index.html) and SWISSPROT databases (http://www.expasy.ch/tools/peptident.htm). Also, the databank of the *P. aeruginosa* genome project was used (http://www. pseudomonas.com).

RESULTS

MucA56 protein is localized to the cytoplasm

MucA56-phoA fusion expression vector pCAQ57 was confirmed first by PCR and sequencing, then by western blot, using anti-alkaline phosphatase antibody. pKMG170 and pKMG176 was constructed by Kalai Mathee, the *mucA-phoA* fusion protein of which was proved to localize to the cytoplasm and periplasm, respectively. Also, their transformants were proved to display white and blue color on L agar containing XP at 40 mg/ml, respectively. pCAQ57, pKMG170 and pKMG176 (PAO1) were tested on L agar containing XP (Figure 1b). As demonstrated previously, the blue color was observed for pKMG176

and white color was observed for pKMG170 (Mathee et al., 1997). Bacteria carrying *mucA56-phoA* fusion expres-
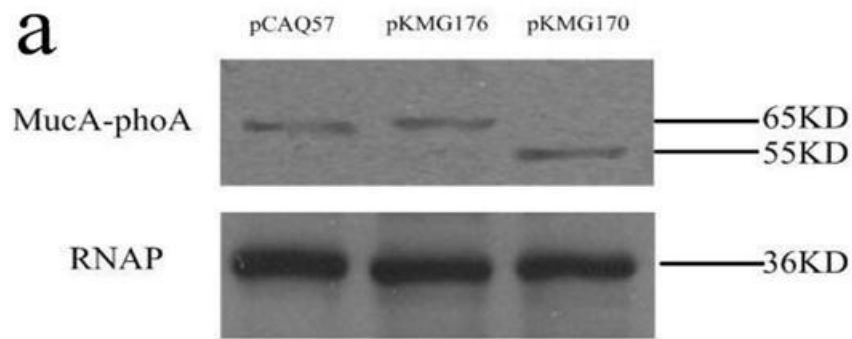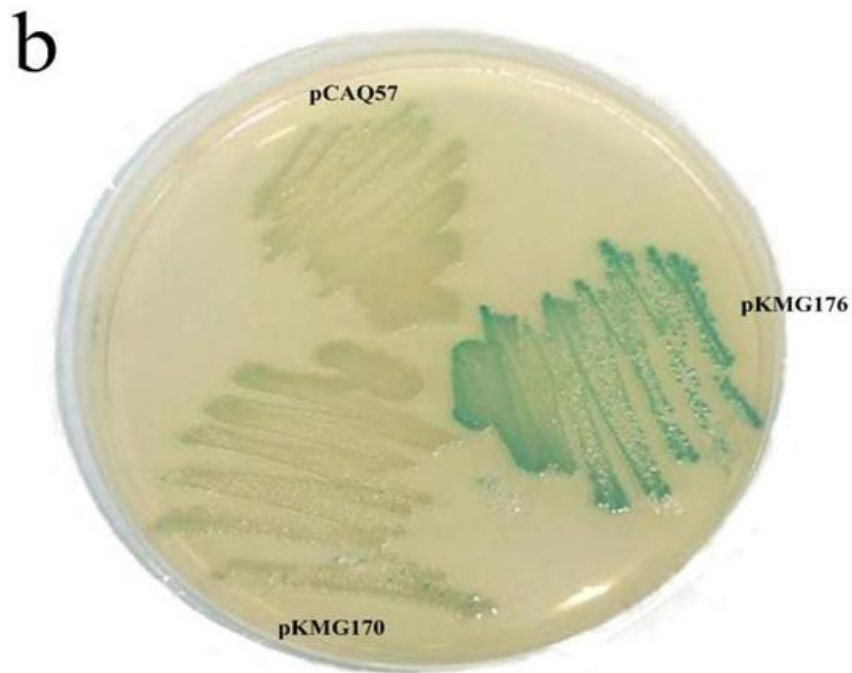
Figure 1. Gene fusion vector pCAQ57, pKMG176 and pKMG170 as confirmed by western blot using anti-alkaline phosphatase antibody. All the three vectors showed the corresponding size of molecular weight (a). PAO1 containing the fusion vectors were tested on L agar containing XP at 40 mg/ml (b). pCAQ57 and pKMG170 displayed white color, while pKMG176 displayed blue color.

sing plasmid pCAQ57 also showed white color analogous to pKMG170, indicating that MucA56 is localized to the cytoplasm.

Construction of a PAO1 derivative with *mucA56* allele, phenotypic characteristics of the strains

PAO*mucA*56 (*mucA56* derivative of PAO1) was generated with gene replacement technique. Colonies exhibiting mucoid phenotype, sucrose resistance and carbenicillin sensitivity were isolated. PDO300 is also an isogenic derivative of PAO1 that was engineered by allelic exchange to contain the *mucA*22 allele, which is characterized by a single base pair deletion at position 430 that causes a premature stop codon. Both PAO*mucA*56 and PDO300 displayed mucoid colony and alginate were overproduced by PDO300 (160 µg alginate ml^{-1}) and PAO*mucA*56 (83 µg alginate ml^{-1}), whereas the parental PAO1 displayed non-mucoid colony and made virtually none (Figure 2).

Effect of *mucA56* mutation on biofilm structures
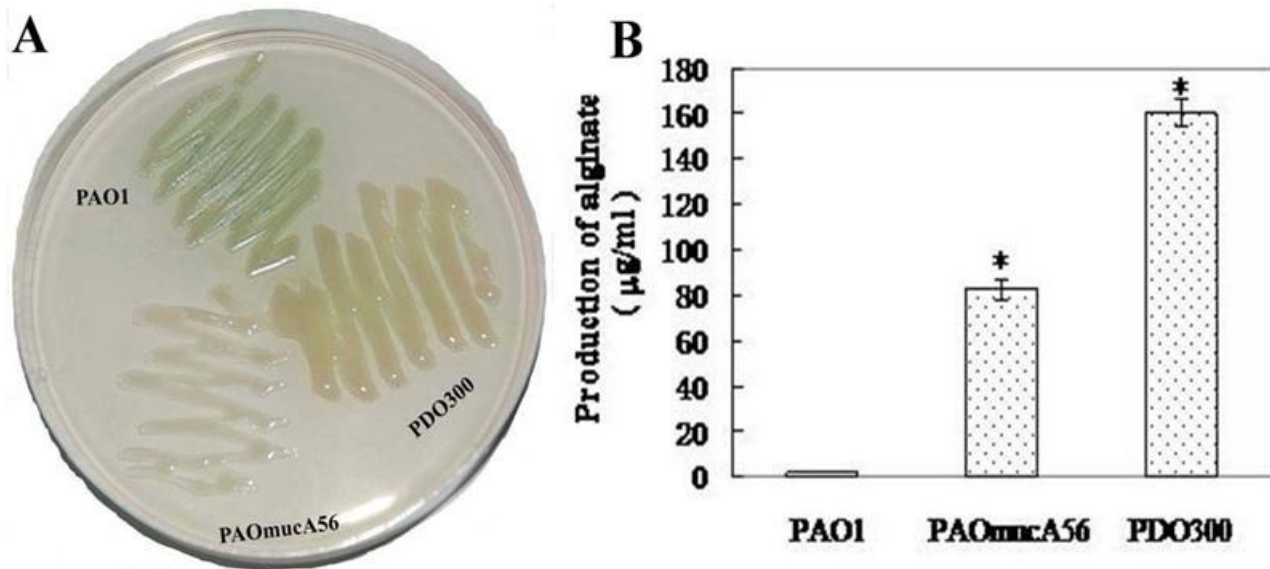
Figure 2. (A) The phenotypes of *P.aeruginosa* strain PAO1, PAO*mucA56,* PDO300 displayed on PIA agar; (B) the alginate production of the three strains.

overproduction of the exopolysaccharide-alginate. However, the alginate production of PDO300 was much more than that of PAO*mucA56*. We wondered whether these differences can influence the biofilm architecture. A plasmid constitutively expressing GFP was introduced into PAO1, PAO*mucA56* and PDO300 strains by electrotransformation. The strains harboring the GFP-expressing plasmid were cultured in a modified continuous-flow biofilm reactor in LB broth, and were then monitored with SCLM. After the initial attachment phase, the biofilm of PAO*mucA56* and PAO1 developed from a relative uniform monolayer of attached cells into a biofilm with little heterogeneity characterized by almost complete substratum coverage. PDO300 formed a significantly different biofilm architecture, which developed from discrete microcolonies of attached cells into a biofilm with low substratum coverage and high structural hetero-geneity (Figure 3).

Protein expression in biofilm cells at different growth phases

Two-dimensional images of crude protein extracts of the three strains are presented in Figure 4. The differently expressed spots whose abundance is same between PAO1 and PAO*mucA56* but different from PDO300, were selected according to the following parameters (smooth, min area, saliency) and then taken for analysis by MALDITOF-MS. The results are listed in Table 2. There were 17 candidate proteins with high reliability, among which the DNA directed RNA polymerase β-subunit, glutamine synthetase, endopeptidase Clp2, elongation

factor Tu , DNA directed RNA polymerase α subunit , elongation factor G1, heat shock protein HtpG , ATP dependent Clp protein ATP binding subunit clpX and trigger factor, are relatively down-regulated in PDO300, while 30S ribosomal protein S18, phosphoenolpy ruvate carboxykinase, dihydrolipoyllysine-residue acetyltrans-ferase component of pyruvate dehydrogenase complex, PasP, biotin carboxylase, arginine deiminase, ornithine carbamoyltransferase and serine hydroxymethyl-transferase 3, are relatively up-regulated in PDO300.

DISCUSSION

A more-or-less permanent chronic colonization was esta-blished upon conversion of *P. aeruginosa* to the mucoid phenotype, and this was also associated with heightened inflammation, tissue destruction, declining pulmonary function, poor progress and higher mortality. The *mucA* mutation is the most important cause of mucoid conversion (Firoved and Deretic, 2003), which is involved in the AlgU (σ^{22}) regulation, the cytoplasmic domain of MucA sequesters σ^{22} in the inner membrane, thus preventing the σ^{22} from binding to promoters. MucB functions as a negative regulator that binds to the peri-plasmic domain of MucA, thus stabilizing this anti - σ factor.

The newly identified *mucA56* gene encoding a cyto-plasm localized MucA56 protein contributed to the instability bond of MucA and AlgU, resulting in the mucoid phenotype of PAO*mucA56*. The C-terminal truncation of MucA protein encoded by *mucA22* contributed to instability bond of MucA and MucB, eventually resulting in

the release of σ[22] and the mucoid phenotype of PDO300.

Both PAO*mucA56* and PDO300 displayed mucoid
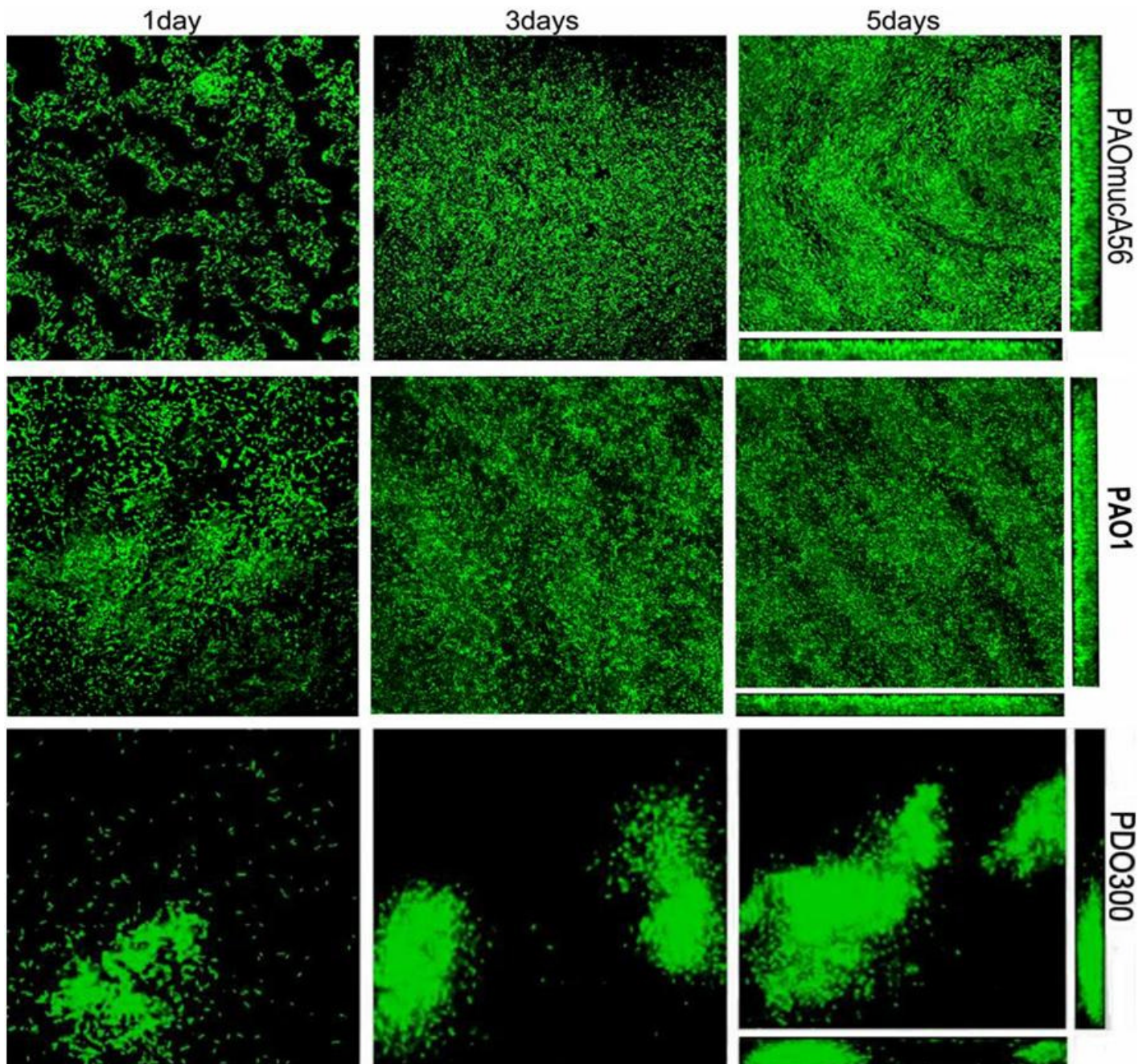
Figure 3. Scanning confocal laser microscopy of the surface-attached communities formed by PAO1, PAO*mucA56* and PDO300. The biofilms are grown in modified flow-through continuous-culture reaction vessels, and the strains tagged with GFP were monitored with CLSM. Scanning confocal photomicrographs of PAO*mucA56*(top), PAO1(middle), PDO300(Bottom); images were acquired at 1day (left), 3 days (middle), 5 days (right) post-inoculation of the biofilm reactor. Vertical sections through the five days biofilms collected at the positions were shown in right and lower frames.

phenotype on PIA agar. However, PDO300 looked more mucoidy and produced more alginate than PAO*mucA56*. Further observation of biofilm architecture revealed that both PAO1 and PAO*mucA56* formed a biofilm characterized by almost complete substratum coverage with mild heterogeneity, while PDO300 formed a biofilm characterized by large microcolonies and a low degree of substratum coverage. We might conclude that the amount of alginate may affect the Pseudomonas aeruginosa biofilm structure, which coincide with previous study (Hentzer et al., 2001). However, the mucoid strain PAO*mucA56* produced a great amount of alginate. The

biofilm development and structure was not affected compared to PAO1. Except for alginate, we speculated
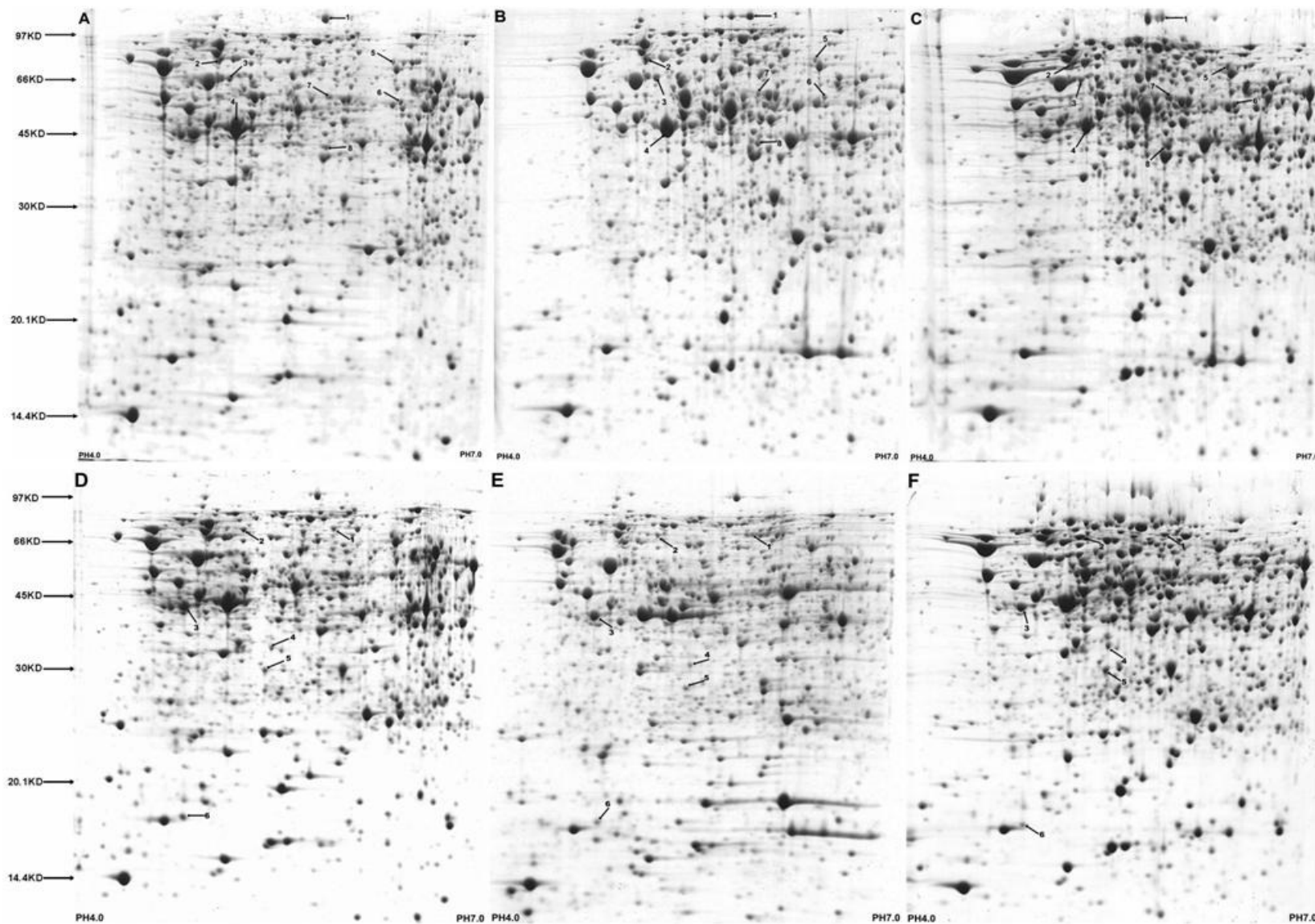
Figure 4. Two-dimensional images of crude protein extracts of PAO1,PAO*mucA56* and PDO300 attached for 1 day (A, B and C, respectively), 3 days (D, E and F, respectively), and 5 days (G, H and I, respectively). The crude protein extracts (1000 µg) were separated on pH 4 to 7 nonlinear Immobiline Dry strips (GE Healthcare; Amersham Biosciences), followed by SDS polyacrylamide gel electrophoresis. Gels were stained with Coomassie brilliant blue R350;arrows pointing indicate proteins that were differentially expressed and were picked up for MS analysis.
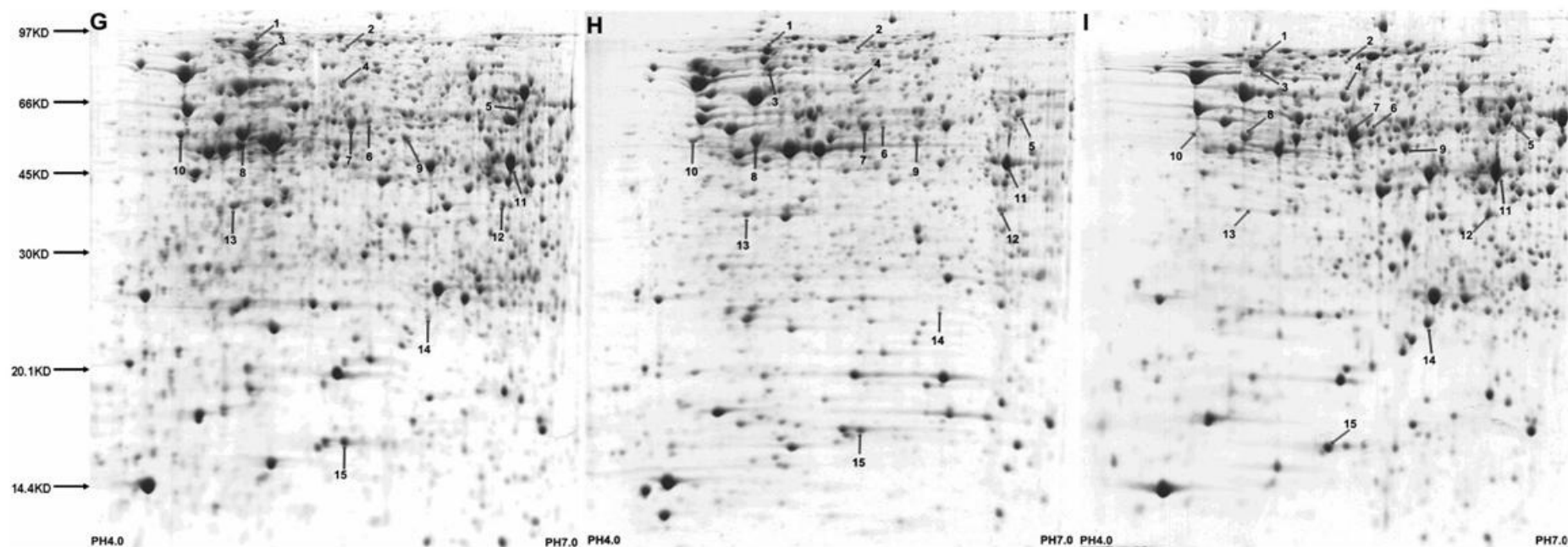
Figure 4. Contd.

that there might be some other factors contributing to the highly structured biofilm in PDO300. As a result, the proteomes of biofilm cells with different ages of the three strains were compared. Proteomes of total protein extract revealed that phosphoenol-pyruvate carboxylase kinase, dihydrolipoyllysine-residue acetyltransferase component of pyruvate dehydrogenase complex and biotin carboxylase were relatively up-regulated in PDO300, and are involved in energy metabolism and also have some impact on biofilm formation. PasP, a secreted factor involved in secretion of toxin, enzymes and alginate, is up-regulated in PDO300, which might be responsible for the highly structured biofilm in PDO300 (Marquart et al., 2005). There are many proteins involved in

carbon catabolism and amino acid metabolism (such as arginine deiminase, ornithine carbamoyl-transferase and serine hydroxymethyltransferase 3), and these were up-regulated in PDO300. Many proteins playing role in transcription, translation and post-translational modification were found to be down-regulated in PDO300, including DNA-directed RNA polymerase subunit beta, elongation factor Tu, DNA-directed RNA polymerase subunit alpha, elongation factor G1, and chaperone protein htpG, trigger factor. The most interesting finding was that two proteins of Clp protease family were both relatively down-regulated in PDO300 on the third and fifth day of biofilm formation. There is evidence that ClpXP-mediated degradation of the cytoplasmic N terminus of RseA to release the sequestered σ^E

into the cytoplasm and the ClpP, ClpX and ClpP2 may play a role in degrading the cytoplasmic region of MucA protein (Qiu et al., 2008). However, whether they take part in the highly structured biofilm and the role they played in the biofilm development need further experiment.

Conclusion

σ^{22}/MucAB play a role in stress response system in *P. aeruginosa* to enable it survive environmental changes. In this study, we focused on *mucA56* and *mucA22* mutation selected by surrounding circumstance. The unique structure of MucA56 protein resulted in mucoid phenotype, but has no effect on biofilm architecture compared to PAO1.

Table 2. Identification of selected protein spots that were differentially expressed over the course of biofilm development.

Time[a]	Locus[b]	Spot	Protein[c]	Mass	PI	MS Score	Fold change[d]	
							A/B	A/C
BF1	PA4270	1	DNA-directed RNA polymerase subunit beta	15.131	5.61	247	0.94	2.03
	PA4761	2	Chaperone prote dnaK	68.405	4.81	42	1.2	1.93
	PA5119	3	Glutamine synthetase	52.140	5.14	219	1.03	1.64
	PA4265	4	Elongation factor Tu	43.684	5.23	161	1.03	1.57
	PA4934	5	30S ribosomal protein S18	87.24	10.61	67	1.14	0.67
	PA5192	6	Phosphoenolpyruvate carboxykinase	56.153	5.27	254	0.84	0.67
	PA3134	7	glutamyl-tRNA synthetase	54.170	5.79	41	0.91	0.64
	PA5500	8	Zincimport ATP-binding protein znuC	29.423	7.82	22	1.03	0.57
BF3	PA1596	1	Chaperone prote htpG	72.577	4.89	55	0.85	0.56
	PA5016	2	Dihydrolipoyllysine-residue acetyltransferase component of pyruvate dehydrogenase complex	56.788	5.23	79	0.89	0.39
	PA4238	3	DNA-directed RNA polymerase subunit alpha	36.741	4.88	91	0.93	1.52
	PA0423	4	PasP	20.764	6.09	69	0.95	0.57
	PA4964	5	topoisomerase IV subunit A	91.434	6.32	42	0.96	0.59
	PA3326	6	probable Clp-family ATP-dependent protease	22.128	5.44	122	0.92	1.51
BF5	PA4266	1	Elongation factor G 1	78.077	5.06	199	0.85	2.73
	PA4761	2	Chaperone protein dnaK	68.405	4.81	42	0.9	1.7
	PA1596	3	Chaperone protein htpG	71.624	5.13	426	1.19	1.86
	PA0519	4	nitrite reductase	65.457	4.83	49	0.94	0.49
	PA0958	5	oprD	48.331	4.96	38	0.93	0.58
	PA4848	6	biotin carboxylase	49.256	5.92	114	0.93	0.6
	PA5171	7	Arginine deiminase	46.806	5.52	272	1.08	0.36
	PA1802	8	ATP-dependent Clp protease ATP-binding subunit ClpX	46.962	5.36	84	0.92	2.74
	PA0770	9	Ribonuclease 3	24.895	6.32	62	0.97	0.46
	PA1800	10	Trigger factor	48.552	4.83	396	0.82	4.51
	PA3537	11	Ornithine carbamoyltransferase	38.255	6.13	102	1.14	0.58
	PA4602	12	Serine hydroxymethyltransferase 3	45.414	5.70	151	1.17	0.48
	PA3744	13	16S rRNA processing protein	18.837	5.69	47	0.84	6.63
	PA4759	14	dihydrodipicolinate reductase	26.652	5.34	53	0.91	0.17
	PA3807	15	nucleoside diphosphate kinase	15.639	5.48	33	0.98	1.72

[a]BF1,BF3,BF5 represent the biofilm formation at one, three, and five days, respectively; [b]the locus designates the gene number according to the *Pseudomonas Genome Project* (http://www.pseudomonas.com); [c]proteins identified by peptide mass fingerprinting; [d]fold change of A/B calculated as the IOD % value of the protein in PAO*mucA56* vs. PAO1, and fold change of A/C calculated as the IOD % value of the protein in PAO*mucA56* vs. PDO300.

However, the special structure of MucA22 protein resulted in mucoid phenotype and high structured biofilm compared to PAO1 and PAO*mucA56*. Also, compared with PAO*mucA56* and PAO1, PDO300 not only produced more alginate, but also had many proteins involved in energy metabolism, carbon catabolism and amino acid metabolism and so on, up-regulated. We might conclude therefore that alginate production may affect biofilm architecture, and except for alginate, many other proteins involved in protein synthesis, MucA degradation, energy metabolism and so on might collectively contribute to the highly structured biofilm of PDO300.

ACKNOWLEDGEMENTS

REFERENCES

Alba BM, Gross CA (2004). Regulation of the Escherichia coli sigma dependent envelope stress response. Mol. Microbiol., 52(3): 613-619.

Bragonzi AL ,Wiehlmann, Klockgether J, Cramer N, Worlitzsch D, Doring G, Tummler B (2006). Sequence diversity of the mucABD locus in Pseudomonas aeruginosa isolates from patients with cystic fibrosis. Microbiology, 152(11): 3261-3269.

Chaba R, Grigorova IL, Flynn JM, Baker TA , Gross CA(2007). Design principles of the proteolytic cascade governing the sigmaE-mediated envelope stress response in Escherichia coli: keys to graded, buffered, and rapid signal transduction. Genes Dev. 21(1): 124-136.

Davies DG, Parsek MR, Pearson JP, Iglewski BH, Costerton JW, Greenberg EP (1998). The involvement of cell-to-cell signals in the development of a bacterial biofilm. Science, 280(5361): 295-298.

Deretic V, Schurr MJ, Boucher JC, Martin DW (1994). Conversion of Pseudomonas aeruginosa to mucoidy in cystic fibrosis: environmental stress and regulation of bacterial virulence by alternative sigma factors. J. Bacteriol., 176(10): 2773-2780.

Firoved AM, Deretic V (2003). Microarray analysis of global gene expression in mucoid Pseudomonas aeruginosa. J. Bacteriol., 185(3): 1071-1081.

Hentzer MG, Teitzel M, Balzer GJ, Heydorn A, Molin S, Givskov M, Parsek MR (2001). Alginate overproduction affects Pseudomonas aeruginosa biofilm structure and function. J. Bacteriol., 183(18): 5395-5401

Knutson CA, Jeanes A (1968). A new modification of the carbazole analysis: application to heteropolysaccharides. Anal. Biochem. 24: 470–481.

Mathee K, Ciofu O, Sternberg C, Lindum PW, Campbell JI, Jensen P, Johnsen AH, Givskov M, Ohman DE, Molin S, Hoiby N, Kharazmi A (1999). Mucoid conversion of Pseudomonas aeruginosa by hydrogen peroxide: a mechanism for virulence activation in the cystic fibrosis lung. Microbiology, 145(6): 1349-1357.

Mathee K McPherson CJ, Ohman DE (1997). Posttranslational control of the algT (algU)-encoded sigma22 for expression of the alginate regulon in Pseudomonas aeruginosa and localization of its antagonist proteins MucA and MucB (AlgN). J. Bacteriol., 179(11): 3711-3720.

Marquart ME, Caballero AR, Chomnawang M, Thibodeaux BA, Twining SS, O'Callaghan RJ (2005). Identification of a novel secreted protease from Pseudomonas aeruginosa that causes corneal erosions. Invest Ophthalmol. Vis Sci., 46(10): 3761-3768.

Ohman DE (2009). Alginate Gene Regulation. Rehm BHA (ed.), Alginates: Biology and Applications, Microbiol. Monographs, 13: 118-128.

Qiu D, Eisinger VM, Head NE, Pier GB, Yu HD (2008). ClpXP proteases positively regulate alginate overexpression and mucoid conversion in Pseudomonas aeruginosa. Microbiology, 154(7): 2119-2130.

Qiu D, Eisinger VM, Rowen DW, Yu HD (2007). Regulated proteolysis controls mucoid conversion in Pseudomonas aeruginosa. Proc. Natl. Acad. Sci. USA. 104(19): 8107-8112.

Karin S, Anne KC, Garth DE, William JC, David GD (2002). Pseudomonas aeruginosa Displays Multiple Phenotypes during Development as a Biofilm. J. Bacteriol., 184(4): 1140–1154.

Stapper AP, Narasimhan G, Ohman DE, Barakat J, Hentzer M, Molin S, Kharazmi A, Hoiby N, Mathee K (2004). Alginate production affects Pseudomonas aeruginosa biofilm development and architecture, but is not essential for biofilm formation. J. Med. Microbiol., 53(7): 679-690.

Stover CK, Pham XQ, Erwin AL, Mizoguchi SD, Warrener P, Hickey MJ, Brinkman FS, Hufnagle WO, Kowalik DJ, Lagrou M, Garber RL, Goltry L, Tolentino E, Westbrock-Wadman S, Yuan Y, Brody LL, Coulter SN, Folger KR, Kas A, Larbig K, Lim R, Smith K, Spencer D, Wong GK, Wu Z, Paulsen IT, Reizer J, Saier MH, Hancock RE, Lory S, Olson MV (2000). Complete genome sequence of Pseudomonas aeruginosa PAO1, an opportunistic pathogen. Nature, 406(6799): 959-964.

Yang Y, Thannhauser TW, Li L, Zhang S (2007). Development of an integrated approach for evaluation of 2-D gel image analysis: impact of multiple proteins in single spots on comparative proteomics in conventional 2-D gel/MALDI workflow. Electrophoresis, 28(12): 2080-2094.

Zhang J, Ma H, Feng J, Zeng L, Wang Z, Chen S (2008). Grape berry plasma membrane proteome analysis and its differential expression during ripening. J. Exp. Bot., 59(11): 2979-2990.